A Comprehensive Two-Way Doppler Noise Model for Near-Real-Time Validation of Doppler Data

A. L. Berman
DSN Network Operations Section

Recent articles have described the functional dependence of plasma-induced doppler noise ("media" noise) upon geometric parameters which approximate integrated signal path electron density (the "ISED" model). In this article, doppler noise generated within the tracking system ("system" noise) is modeled as a function of the dominant variable – doppler sample interval. Additionally, the relationship between media noise and doppler sample interval is empirically determined, and the ratio of media noise for S- and X-band downlinks is solved for. These functional relationships are incorporated into the previous media noise modeling to obtain a comprehensive two-way doppler noise model – ISEDC.

I. Introduction

Doppler noise has for some time been considered the strongest indicator of tracking system performance, and nothing appears likely to soon usurp that position. Doppler noise can be conveniently divided into two broad and very different categories: noise generated within the tracking system ("system" noise) and noise induced by the media being traversed ("media" noise). The last two years have seen an intensive effort mounted to model media noise (the ISED model; see Refs. 1-6). The reason why resources were first directed towards modeling the media noise is apparent from a comparison of the regions of interest for system noise and media noise, here roughly considered to be (rms phase jitter):

$$10 \text{ deg} \lesssim \text{system noise} \lesssim 100 \text{ deg}$$

$$100 \text{ deg} \lesssim \text{media noise} \lesssim 100{,}000 \text{ deg}$$

or for 60-second sample interval noise[1]:

$$0.0005 \text{ Hz} \lesssim \text{system noise} \lesssim 0.005 \text{ Hz}$$

$$0.005 \text{ Hz} \lesssim \text{media noise} \lesssim 5.000 \text{ Hz}$$

Obviously, modeling media noise was a higher priority as it occupies the highest three orders of magnitude of the four orders of magnitude that doppler noise is commonly observed to span. With the media noise modeling nearing completion, it seems appropriate to address the question of system noise modeling.

[1]For convenience, all expressions in rms phase jitter (degrees) will also be given in equivalent 60-second sample interval noise (Hz).

The most important functional parameter which describes system noise is doppler sample interval, and, therefore, tests were conceived and executed to empirically obtain this relationship. In addition, the relationship between media noise and doppler sample interval is obtained, as is the ratio of media noise for S-band and X-band downlinks. Finally, these relationships are incorporated into the ISED media noise model to yield a comprehensive two-way doppler noise model.

II. Tracking System Doppler Noise Dependence Upon Doppler Sample Interval

The only doppler system noise model known to DSN Network Operations, since at least the beginning of this decade, is as follows:[2]

$$\text{Rms phase jitter} = \left\{(B_0 + C_0)^2\,\tau^2 + (B_1 + C_1)^2 + \frac{(B_2 + C_2)^2}{(B_3 + C_3)^2}\right\}^{1/2}$$

or

$$\text{Noise} = \left\{(B'_0 + C'_0)^2 + \frac{(B'_1 + C'_1)^2}{\tau^2} + \frac{(B'_2 + C'_2)^2}{(B'_3 + C'_3)^2\,\tau^2}\right\}^{1/2}$$

where

B_n, B'_n = tracking station constants

C_n, C'_n = spacecraft constants

τ = doppler sample interval, seconds

However, no values for the constants were ever determined (or if they were, they certainly have not survived!) and so this formulation is of little inherent interest. Since the most important parameter for system noise is the doppler sample interval, it was felt that a reasonable starting point would be an (empirical) investigation of doppler noise variation with sample interval, for spacecraft *not* in solar conjunction phases.

A. System Noise as a Function of Doppler Sample Interval

Four spacecraft not currently in solar conjunction phases were available for doppler noise variation with sample interval tests:

Pioneer 10
Pioneer 11
Helios 1
Helios 2

For each spacecraft, four tests (on different passes) were conducted to obtain typical variations of noise with sample interval. In each test, essentially 150 doppler samples[3] were used to obtain an "average" doppler noise value for the following doppler sample intervals:

1 second
2 seconds
5 seconds
10 seconds
20 seconds
60 seconds

The signatures obtained for the four spacecraft were quite different, but all showed a small to moderate increase in phase jitter with doppler sample interval:

$$\text{Rms phase jitter} \sim \tau^{0.1\,-\,0.2}$$

or

$$\text{Noise} \sim \frac{1}{\tau^{0.8\,-\,0.9}}$$

That the noise versus sample interval signatures were quite different is not surprising as many factors enter into the process, such as:

(1) Spacecraft characteristics (spin, transponder, receiver/transmitter).

(2) Frequency standard, combined with τ.

(3) Doppler extractor, combined with signal level.

[2] This model was used in the DSN IBM 360 era (1970-1975) and remains in the MCCC Pseudo-Residual Program.

[3] Obtained by averaging 10 noise calculations, each noise calculation derived from 15 samples.

(4) Doppler resolver quantization, combined with doppler level.

All available evidence appears to point to the first two as the major contributors to system noise (the "system" noise definition here broadened to include both ground and spacecraft systems, i.e., everything but "media" noise). There exists a persistent misconception that signal level plays an important part in modeling doppler noise – this having been empirically demonstrated by the author not to be true with actual Mariner 9 data (Ref. 7) in 1972. The unimportance of signal level (except in cases where there exists less than 10 dB of margin above threshold) can also be seen in a system noise model constructed by W. D. Chaney (Ref. 8) from tracking subsystem performance parameters, as follows (when RTLT $> \tau$):

Rms phase jitter, cycles

$$= \left\{ [2\sigma_R{}^2 + 2\sigma_Q{}^2 + 2\sigma_T{}^2] + \left[\frac{\Delta f}{f}(2.3 \times 10^9)\tau\right]^2 + \left[\frac{\Delta\phi}{\Delta T}\tau\right]^2 \right\}^{1/2}$$

where

σ_R = receiver phase jitter $\approx$ 0.019 cycle under strong signal

σ_Q = resolver quantization $\approx$ 0.01 cycle

σ_T = 1-pulse/second timing jitter $\approx$ 0.04 cycle

$\Delta f/f$ = rubidium frequency stability $\approx 1 \times 10^{-12}$ to 5×10^{-12}

$\Delta\phi/\Delta t$ = station phase stability $\approx 1.5 \times 10^{-4}$

Except at very low signal levels (less than 10 dB above threshold, other terms, particularly $\Delta f/f$ at the normal 60-second sample interval, obviously predominate over the signal level dependent term – σ_R. In a subsequent section, the "Chaney" formulation will be compared to the actual results obtained.

B. System Noise Versus Sample Interval Test Results

Initial examination of the data indicated that a general expression of the form:

$$\text{Rms phase jitter, deg} = \left\{ \left[D_0 \left(\frac{\tau}{60}\right) \right]^2 + \left(D_1 \tau^{D_2} \right)^2 \right\}^{1/2}$$

or

$$\text{Noise, Hz} = \left\{ (D_0')^2 + \left[D_1' \left(\frac{60}{\tau}\right)^{D_2'} \right]^2 \right\}^{1/2}$$

where

D_n, D_n' = empirically determined constants

would yield a satisfactory representation for the test data. Individual spacecraft test results are described below.

1. Pioneer 10. Figure 1 presents the sample interval test results for the Pioneer 10 spacecraft; a reasonable fit to these data was obtained as:

$$\text{Rms phase jitter} = 36\ \{\tau\}^{0.1},\ \text{deg}$$

or

$$\text{Noise} = 0.0025 \left\{\frac{60}{\tau}\right\}^{0.9},\ \text{Hz}$$

2. Pioneer 11. Figure 2 presents the sample interval test results for the Pioneer 11 spacecraft; these results were similar to those obtained for Pioneer 10, but at an elevated level:

$$\text{Rms phase jitter} = 48\ \{\tau\}^{0.1},\ \text{deg}$$

or

$$\text{Noise} = 0.0033 \left\{\frac{60}{\tau}\right\}^{0.9},\ \text{Hz}$$

3. Helios 1. Figure 3 presents sample interval test results for the Helios 1 spacecraft. These data were not as amenable to fit as were the Pioneer data, and the results at the larger sample intervals (20 seconds and particularly 60 seconds) are at least twice what routine experience dictates. This is

partially explained by the fact that DSS 44, which provided all of the sample interval tests for Helios 1, was subsequently found to be perhaps 30-50 percent noisier than the other DSSs. This can be easily seen by comparing the one Helios 2-DSS 44 test case (Fig. 4d) to the other three Helios 2 test cases (Figs. 4a, b, c). At any rate, a fair fit to the Helios 1 data, but biased lower because of the DSS 44 (Australia) above-average noise, and biased towards the expected 60-second performance, is:

$$\text{Rms phase jitter} = 24\ \{\tau\}^{0.2},\ \text{deg}$$

or

$$\text{Noise} = 0.0025\ \left\{\frac{60}{\tau}\right\}^{0.8},\ \text{Hz}$$

4. Helios 2. Figure 4 presents sample interval data for the Helios 2 spacecraft. These data were notable for being so low, particularly at the smaller sample intervals. The lowest 1-second sample interval data (DSS 14, Goldstone, Fig. 4a) indicated an rms phase jitter of only 10 degrees!

It was found necessary to add a small linear term in τ to the phase jitter to bring the expression, when evaluated at $\tau = 60$ seconds, up to more commonly experienced results:

$$\text{Rms phase jitter} = \left\{(12\ \{\tau\}^{0.2})^2 + \left(30\left\{\frac{\tau}{60}\right\}\right)^2\right\}^{1/2},\ \text{deg}$$

or

$$\text{Noise} = \left\{\left(0.0013\ \left\{\frac{60}{\tau}\right\}^{0.8}\right)^2 + (0.0014)^2\right\}^{1/2},\ \text{Hz}$$

The results for all four spacecraft are summarized in Table 1.

Based on the different spacecraft characteristics and the radically different RTLTs, it seems reasonable to accept large differences between the Pioneer spacecraft and the Helios spacecraft. There is much less reason to think the smaller differences obtained between Pioneers 10 and 11 and, likewise, between Helios 1 and 2 are significant or that these differences could be confidently predicted into the future. It would seem to make more sense to average the Pioneer 10 and 11 results, and, similarly, the Helios 1 and 2 results. For future doppler noise modeling, a "Pioneer" and "Helios" model will be adopted as follows:

Pioneer

$$\text{rms phase jitter} = 42\ \{\tau\}^{0.1},\ \text{deg}$$

$$\text{Noise} = 0.0029\left\{\frac{60}{\tau}\right\}^{0.9},\ \text{Hz}$$

Helios

$$\text{rms phase jitter} = \left[\left(18\ \{\tau\}^{0.2}\right)^2 + \left(30\left\{\frac{\tau}{60}\right\}\right)^2\right]^{1/2},\ \text{deg}$$

$$\text{Noise} = \left[\left(0.0019\left\{\frac{60}{\tau}\right\}^{0.8}\right)^2 + (0.0014)^2\right]^{1/2},\ \text{Hz}$$

Figure 5 presents these expressions as compared to the Chaney formulation for the following parameter values:

$$\sigma_R = 0.019\ \text{cycle}$$

$$\sigma_Q = 0.010\ \text{cycle}$$

$$\sigma_T = 0.040\ \text{cycle}$$

$$\Delta f/f = 1 \times 10^{-12}$$

$$\Delta\phi/\Delta T = 1.5 \times 10^{-4}.$$

Additionally, included in Fig. 5 for comparison are results obtained by M. Brockman (Ref. 9) for the following conditions:

Frequency standard	= rubidium
Doppler extractor phase noise	= 22 degrees
Timing jitter on doppler sampling	= 5×10^{-9} second
Doppler resolver counter quantization	= 2×10^{-9} second

Considering that this is the first serious attempt to obtain an operational modeling of system noise as a function of sample interval, the correspondence between the Chaney formulation, the Brockman data, and the empirically derived formulations presented here is considered favorably.

III. Plasma-Induced Doppler Noise Dependence Upon Doppler Sample Interval

In July 1976, an initial study was conducted to ascertain the dependence of solar plasma-induced doppler noise upon doppler sample interval, using low Sun-Earth-probe (SEP) doppler noise data from the April-May 1976 solar conjunction of the Helios 2 spacecraft. At that time, a relationship was hypothesized as follows:

$$\frac{\text{Noise } (\tau_2)}{\text{Noise } (\tau_1)} = \left(\frac{\tau_1}{\tau_2}\right)^x$$

where

τ = doppler sample interval

Solving for the exponent (x) in 12 cases where different doppler sample intervals were available at (approximately) the same SEP, a mean value of x was determined as follows:

$$x = 0.285$$

with a standard deviation over the 12 cases of:

$$\sigma(x) = 0.120$$

The recent solar conjunction of the four Viking spacecraft afforded an opportunity to retest the (sample interval dependence) hypothesis, and it was considered reasonable to utilize this opportunity.

Thirty sets of different doppler sample intervals at approximately the same time (hence, SEP) were identified, with the following sample interval comparisons available:

1 second/10 seconds
1 second/60 seconds
2 seconds/10 seconds
10 seconds/60 seconds

The same hypothesis applied to the Helios 2 data was applied to the 30 Viking cases, and the results are seen in Table 2. These cases produced an average value for the exponent (x) of:

$$x = 0.294$$

and a standard deviation of:

$$\sigma\ (x) = 0.106$$

Although, the standard deviation of the exponent solutions is large (as was the case with the Helios 2 data), the average values produced by the Helios 2 data and the subsequent Viking data are extremely close. It should, of course, be cautioned that the results are partially dependent upon the type of processing done in the Network Operations Control Center (NOCC) Pseudo-Residual Program.[4]

For future modeling of doppler noise during solar conjunction periods, the following exponent value (x) will be adopted:

$$x = 0.3$$

so that plasma-induced doppler noise ("ISED") will be scaled by:

$$\left(\frac{60}{\tau}\right)^{0.3}$$

where

τ = doppler sample interval

IV. Plasma-Induced Doppler Noise Dependence Upon Downlink Frequency

A great deal of S- and X-band doppler (and, hence, doppler noise statistics) has been accumulated during the recent Viking solar conjunction phase. Using the inverse proportionality between plasma-induced phase error and frequency, it is easy to derive an expected ratio of X-band doppler noise to S-band doppler noise. It would then seem reasonable to see how close the actual Viking X-band/S-band doppler noise ratio is to the calculated expression.

A. Expected X-band/S-band Doppler Noise Ratio

One begins by defining the following frequencies and frequency ratios:

f_{sup} = S-band uplink frequency (2113 MHz)

[4] The doppler noise computed in the NOCC Pseudo-Residual Program is a "running" standard deviation of the most recent 15 samples calculated about a linear curve to these samples (residuals).

f_{sdn} = S-band downlink frequency (2295 MHz)

f_{xdn} = X-band downlink frequency (8415 MHz)

f_{sdn}/f_{sup} = 240/221

f_{xdn}/f_{sdn} = 11/3

From Ref. 10, one has the phase error caused by fluctuating electron density:

$$\Delta\phi = r_e \lambda n \Delta z$$

$$= r_e \left(\frac{c}{f}\right) n \Delta z$$

where

$\Delta\phi$ = phase error

r_e = classical electron radius

$= 2.8 \times 10^{-18}$ km

λ = wavelength

c = speed of light

f = frequency, Hz

n = electron density

Δz = region containing electron density

Now consider:

$$r_e c n \, \Delta z = K_1$$

so that:

$\Delta\phi_{sup}$ = S-band uplink phase error

$= K_1/f_{sup}$

$\Delta\phi_{sdn}$ = S-band downlink phase error

$= K_1/f_{sdn}$

$\Delta\phi_{xdn}$ = X-band downlink phase error

$= K_1/f_{xdn}$

To calculate the ratio of X-band doppler noise to S-band doppler noise, the following assumptions are made:

(1) If fluctuations in electron density are proportional to electron density, then rms phase jitter will be proportional to the phase error expression from Ref. 10.

(2) "Total" phase jitter on the downlink can be obtained by root sum squaring (rss) the phase jitter induced on the uplink (multiplied to downlink level) with the phase jitter induced on the downlink.

Using the above (with the constant of proportionality between noise and phase error = K_2), one constructs an expression for S-band noise:

$$\text{Noise}_s = K_2 \left[(\Delta\phi_{sup})^2 (240/221)^2 + (\Delta\phi_{sdn})^2 \right]^{1/2}$$

$$= K_2 \left[(K_1/f_{sup})^2 (240/221)^2 + (K_1/f_{sdn})^2 \right]^{1/2}$$

$$= K_1 K_2 \left[(1/f_{sup})^2 (240/221)^2 + (1/f_{sdn})^2 \right]^{1/2}$$

and for X-band noise:

$$\text{Noise}_x = K_2 \left[(\Delta\phi_{sup})^2 (240/221)^2 (11/3)^2 + (\Delta\phi_{xdn})^2 \right]^{1/2}$$

$$= K_2 \left[(K_1/f_{sup})^2 (240/221)^2 (11/3)^2 + (K_1/f_{xdn})^2 \right]^{1/2}$$

$$= K_1 K_2 \left[(1/f_{sup})^2 (240/221)^2 (11/3)^2 + (1/f_{xdn})^2 \right]^{1/2}$$

The ratio is then obtained:

$$\frac{\text{Noise}_x}{\text{Noise}_s} = \frac{\left[(1/f_{sup})^2 (240/221)^2 (11/3)^2 + (1/f_{xdn})^2 \right]^{1/2}}{\left[(1/f_{sup})^2 (240/221)^2 + (1/f_{sdn})^2 \right]^{1/2}}$$

$$= \frac{\left[(240/221)^2\,(11/3)^2 + (f_{sup}/f_{xdn})^2\right]^{1/2}}{\left[(240/221)^2 + (f_{sup}/f_{sdn})^2\right]^{1/2}}$$

$$= \frac{\left[(240/221)^2\,(11/3)^2 + (221/240)^2\,(3/11)^2\right]^{1/2}}{\left[(240/221)^2 + (221/240)^2\right]^{1/2}}$$

$$= \frac{\left[(240/221)^2\,(11/3)^2 + (240/221)^{-2}\,(11/3)^{-2}\right]^{1/2}}{\left[(240/221)^2 + (240/221)^{-2}\right]^{1/2}}$$

Now the X-band noise computed by the Network Operations Control Center (NOCC) RTM is scaled by the downlink S/X ratio:

$$\text{Noise}'_x = \left\{\frac{3}{11}\right\} \text{noise}_x$$

so that the ratio of X-band noise to S-band noise as computed by the RTM would be:

$$\frac{\text{Noise}'_x}{\text{Noise}_s} = \frac{3}{11}\,\frac{\left[(240/221)^2\,(11/3)^2 + (240/221)^{-2}\,(11/3)^{-2}\right]^{1/2}}{\left[(240/221)^2 + (240/221)^{-2}\right]^{1/2}}$$

$$= 0.764$$

B. Measured Ratio of X-Band to S-Band Doppler Noise

During the period from 1 July 1976 to 1 October 1976, frequent measurements of the X-band to S-band doppler noise ratio were recorded. The measurements were made for doppler data taken at the 64-meter stations, and, in all cases, were made for identical 15-minute time periods of 60-second sample interval data. The only constraint imposed was that the S-band noise be greater than 0.010 Hz, so as to minimize the non-plasma component of the doppler noise. A total of 405 measurements, equivalent to a total of 101 hours, were recorded during the 1 July-1 October period, and these measurements yielded a composite average of (with X-band "normalized" to S-band level):

$$\frac{\text{Noise}'_x}{\text{Noise}_s} = 0.704$$

The difference between the measured value (above) and the predicted value from Section II is about 8 percent:

$$\frac{\text{Measured ratio}}{\text{Predicted ratio}} \approx 0.92$$

For future doppler noise modeling, the following will be adopted (with X-band noise "normalized" to S-band level):

$$\frac{\text{Noise}'_x}{\text{Noise}_s} = 0.7$$

V. A Composite Two-Way Doppler Noise Model

Combining the results from the previous three sections with the ISEDB (Refs. 1 and 2) model, one has (the "ISEDC" model):

$$\text{ISEDC, Hz} = \left[\left(\left\{A_0\left[\frac{\beta}{(\sin\alpha)^{1.3}}\right]F(\alpha,\beta) + A_1\left[\frac{1}{(\sin\alpha)^5}\right]\right\} 10^{-A_8(|\phi_s|/90)}\right)^2 \times (K(f_{dn}))^2\left(\left\{\frac{60}{\tau}\right\}^{0.3}\right)^2 + (D'_0)^2 + \left(D'_1\left\{\frac{60}{\tau}\right\}^{D'_2}\right)^2\right]^{1/2}$$

where

f_{dn} = downlink frequency (S- or X-band)

$$K(f_{dn}) = \begin{cases} 1.0 & f_{dn} = \text{S-band} \\ 0.7 & f_{dn} = \text{X-band} \end{cases}$$

τ = doppler sample interval, seconds

$$D'_0 = \begin{cases} 0 & \text{Pioneer spacecraft} \\ 0.0014 & \text{Helios spacecraft} \end{cases}$$

$$D'_1 = \begin{cases} 0.0029 & \text{Pioneer spacecraft} \\ 0.0019 & \text{Helios spacecraft} \end{cases}$$

$$D'_2 = \begin{cases} 0.9 & \text{Pioneer spacecraft} \\ 0.8 & \text{Helios spacecraft} \end{cases}$$

$$F(\alpha,\beta) = 1 - 0.05\left\{\frac{(\beta - \pi/2 + \alpha)^3 - (\alpha - \pi/2)^3}{\beta}\right\} - 0.00275\left\{\frac{(\beta - \pi/2 + \alpha)^5 - (\alpha - \pi/2)^5}{\beta}\right\}$$

α = Sun-Earth-probe angle (SEP), radians

β = Earth-Sun-probe angle (ESP), radians

and

ϕ_s = heliographic latitude, degrees

$= \sin^{-1} [\cot \alpha (-\cos \delta_d \sin \alpha_{ra} \sin \epsilon + \sin \delta_d \cos \epsilon)]$

α_{ra} = right ascension

δ_d = declination

ϵ = the obliquity of the ecliptic (23.445 deg)

with

$A_0 = 9.65 \times 10^{-4}$

$A_1 = 5 \times 10^{-10}$

$A_8 = 9 \times 10^{-1}$

VI. Summary

The dependence upon doppler sample interval of both the media and system components of doppler noise has been empirically deduced from actual data and appropriately modeled. Additionally, the ratio of media noise for X-band downlinks as compared to S-band downlinks has been solved for and is shown to be in reasonable agreement with observations. These functional relationships are combined with previous media noise modeling (ISEDB) to obtain a comprehensive two-way doppler noise model – ISEDC. This model greatly enhances DSN capability to predict two-way doppler noise levels for a great variety of circumstances.

References

1. Berman, A. L., Wackley, J. A., and Rockwell, S. T., "The 1976 Helios and Pioneer Solar Conjunctions – Continuing Corroboration of the Link Between Doppler Noise and Integrated Signal Path Electron Density," in *The Deep Space Network Progress Report 42-36,* pp. 121-137, Jet Propulsion Laboratory, Pasadena, California, December 15, 1976.

2. Berman, A. L., Wackley, J. A., Rockwell, S. T., and Yee, J. G., "The Pioneer 11 1976 Solar Conjunction: A Unique Opportunity to Explore the Heliographic Latitudinal Variations of the Solar Corona," in *The Deep Space Network Progress Report 42-35,* pp. 136-147, Jet Propulsion Laboratory, Pasadena, California, October 15, 1976.

3. Berman, A. L., and Wackley, J. A., "Doppler Noise Considered as a Function of the Signal Path Integration of Electron Density," in *The Deep Space Network Progress Report 42-33,* pp. 159-193, Jet Propulsion Laboratory, Pasadena, California, June 15, 1976.

4. Berman, A. L., "Analysis of Solar Effects Upon Observed Doppler Data Noise During the Helios 1 Second Solar Conjunction," in *The Deep Space Network Progress Report 42-32,* pp. 262-276, Jet Propulsion Laboratory, Pasadena, California, April 15, 1976.

5. Berman, A. L., and Rockwell, S. T., "Correlation of Doppler Noise During Solar Conjunctions with Fluctuations in Solar Activity," in *The Deep Space Network Progress Report 42-30,* pp. 264-272, Jet Propulsion Laboratory, Pasadena, California, December 15, 1975.

6. Berman, A. L., and Rockwell, S. T., "Analysis and Prediction of Doppler Noise During Solar Conjunctions," in *The Deep Space Network Progress Report 42-30,* pp. 230-263, Jet Propulsion Laboratory, Pasadena, California, December 15, 1975.

7. Berman, A. L., "Mariner 9 Doppler Noise Study," in *The Deep Space Network Progress Report,* Technical Report 32-1526, Vol. XIII, pp. 227-235, Jet Propulsion Laboratory, Pasadena, California, February 15, 1973.

8. Private communication with W. D. Chaney.

9. Brockman, M. H., "Revision to TRK-20," *Deep Space Network/Flight Project Interface Design Handbook,* Document 810-5, Rev. D, to be published (JPL internal document).

10. Cronyn, W. M., "The Analysis of Radio Scattering and Space-Probe Observations of Small-Scale Structure in the Interplanetary Medium," *Astrophys. J.* Vol. 161, pp. 755-763, August 1, 1970.

Table 1. System noise versus sample interval test results

Parameter	Pioneer 10	Pioneer 11	Helios 1	Helios 2
RTLT, s	10,850	3600	350	150
Spacecraft spin	Yes	Yes	No[a]	No[a]
D_0, deg	0	0	0	30
D_0', Hz	0	0	0	0.0014
D_1, deg	36	48	24	12
D_1', Hz	0.0025	0.0033	0.0025	0.0013
D_2	0.1	0.1	0.2	0.2
D_2'	0.9	0.9	0.8	0.8

[a]At least insofar as any appreciable effect in the doppler is concerned.

Table 2. Viking solar conjunction doppler noise exponent solutions for different sample intervals

Day of year	Spacecraft	Sample intervals, seconds/seconds	x
309	VO1, VO2	10/60	0.392
310	VO1, VO2	10/60	0.196
310	VO1, VO2	10/60	0.249
311	VO1, VO2	10/60	0.305
312	VO1, VO2	10/60	0.159
313	VO1, VO2	10/60	0.249
314	VO1, VO2	10/60	0.177
314	VO1, VO2	10/60	0.126
315	VO1, VO1	10/60	0.221
319	VO1, VO2	10/60	0.098
320	VO1, VO2	10/60	0.258
320	VO1, VO1	10/60	0.299
321	VO2, VO2	2/10	0.333
321	VO2, VL2	2/10	0.526
323	VO2, VL2	2/10	0.478
324	VO1, VO2	10/60	0.225
325	VO1, VL2	2/10	0.332
326	VO2, VL2	2/10	0.285
326	VL2, VL2	2/10	0.226
333	VO1, VL1	1/10	0.329
333	VL1, VL1	1/10	0.264
334	VO1, VL1	1/60	0.391
334	VO1, VL1	1/10	0.310
334	VO1, VO1	10/60	0.500
335	VO1, VL1	1/10	0.339
337	VO1, VL1	1/10	0.400
338	VO1, VL1	1/10	0.408
339	VO2, VL1	1/10	0.328
340	VO2, VL1	1/10	0.187
341	VO2, VL1	1/10	0.245

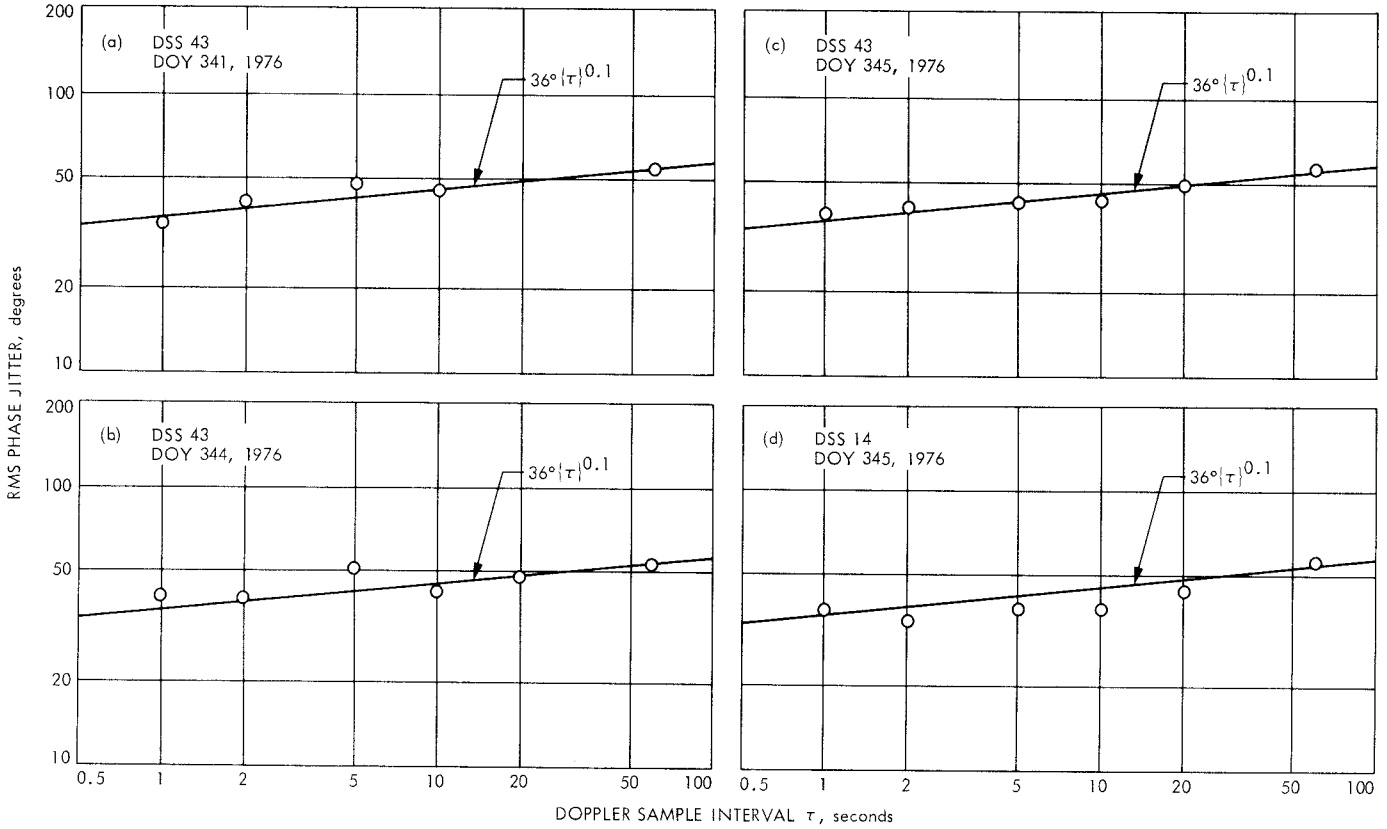

Fig. 1. Pioneer 10 rms phase jitter versus doppler sample interval

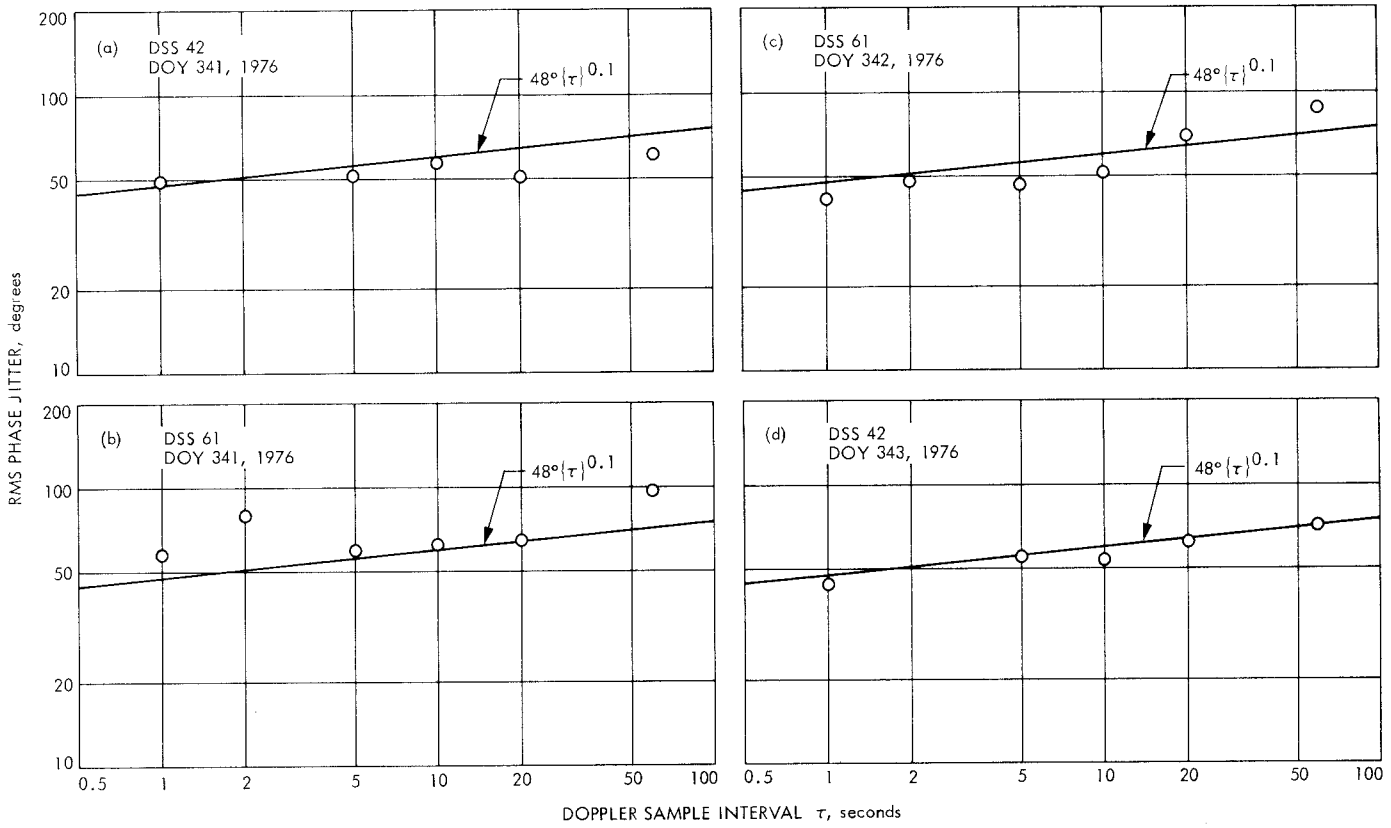

Fig. 2. Pioneer 11 rms phase jitter versus doppler sample interval

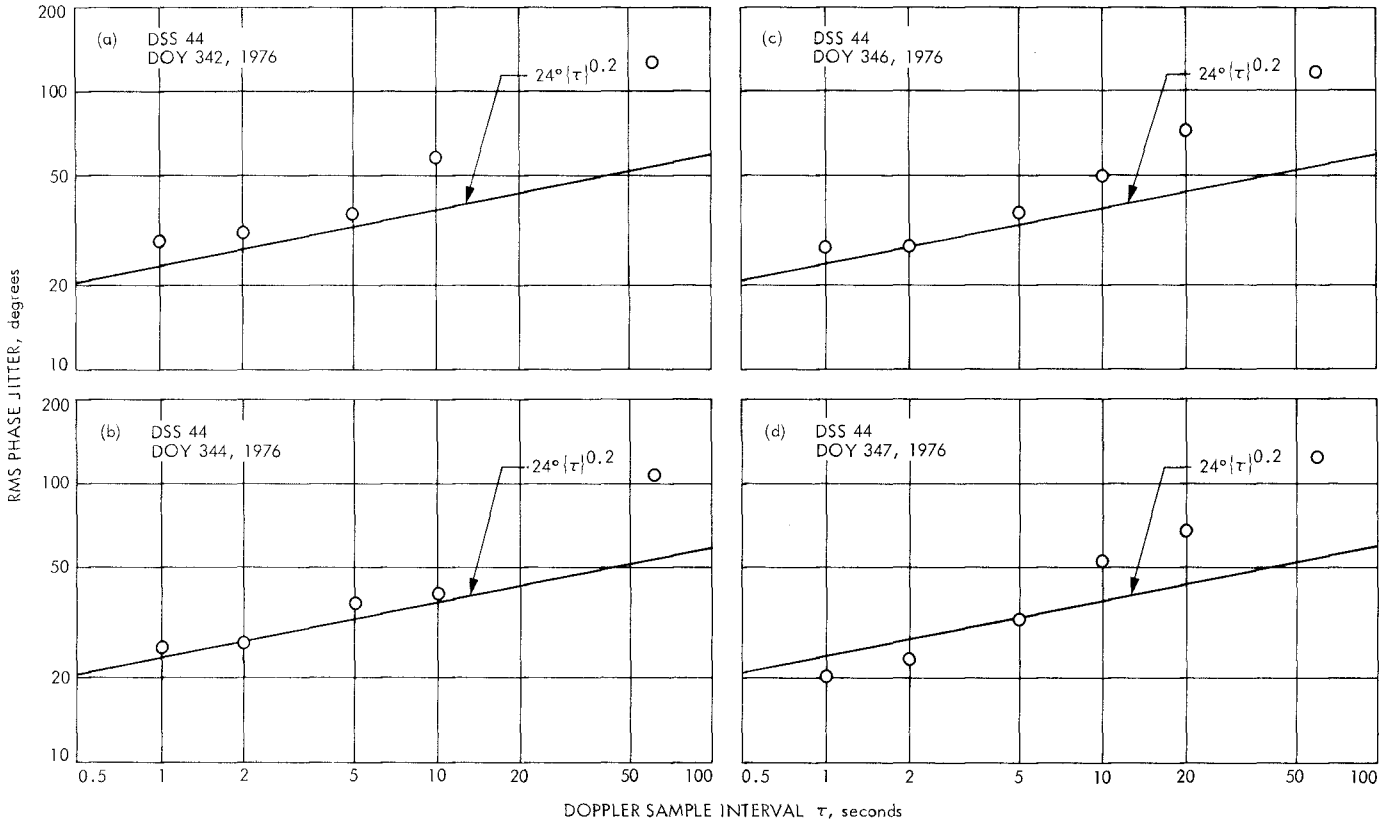

Fig. 3. Helios 1 rms phase jitter versus doppler sample interval

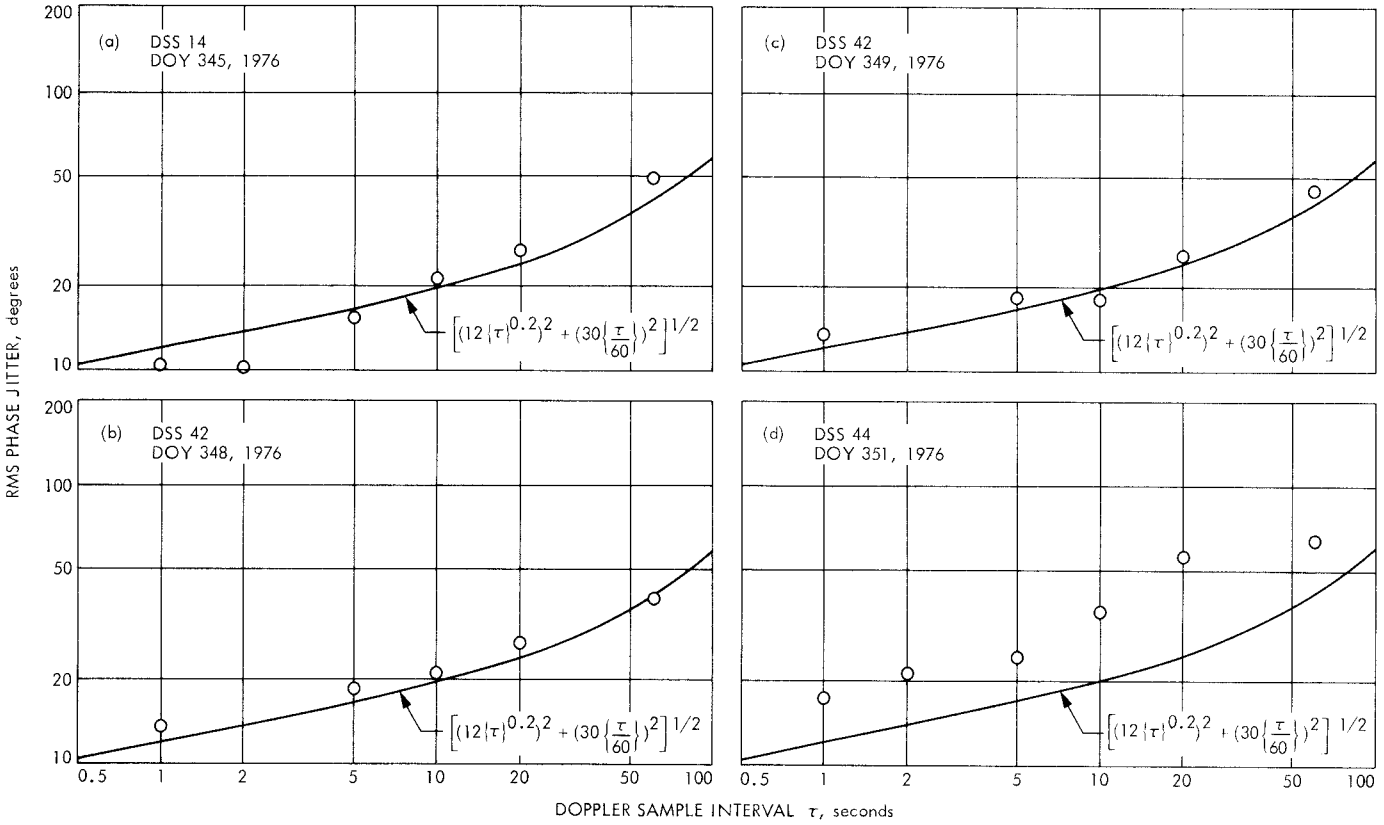

Fig. 4. Helios 2 rms phase jitter versus doppler sample interval

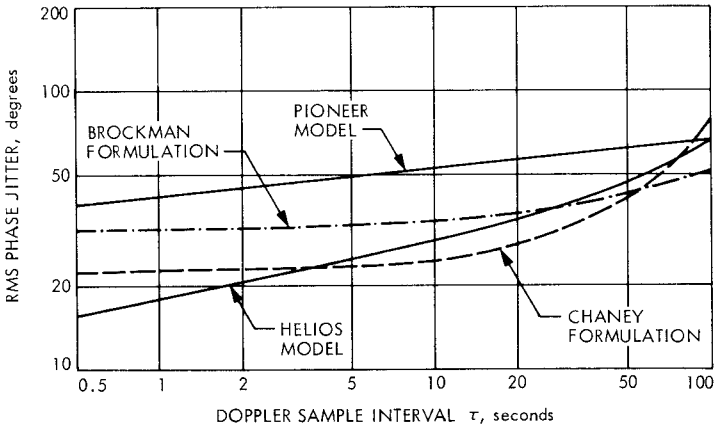

Fig. 5. Doppler system noise model comparisons